C Journal of Carbon Research

MDPI

Article

Synthetic Pitch from Solvent Extraction of Coal as a Source for High-Quality Graphite

Akshay Gharpure *, Randy L. Vander Wal and Sarma Pisupati

Center for Critical Minerals (C^2M), John and Willie Leone Family Department of Energy and Mineral Engineering, EMS Energy Institute, The Pennsylvania State University, University Park, PA 16802, USA
* Correspondence: apg86@psu.edu

Abstract: This work evaluates the potential for obtaining graphitizable precursors from domestically available coal as a possible solution to the declining availability of high-quality precursors and projected rapid growth driven by demand for synthetic graphite in the US. The graphitizability of a coal-derived synthetic pitch (Synpitch) obtained by a novel solvent extraction process is compared with a commercially available petroleum pitch. The process outlined in this paper offers the advantages of lower temperature, pressure, and hydrogen addition requirement. An upgraded (higher H/C) aromatic pitch with low quinoline insoluble (QI) and ash content is obtained. The distinctions between the pitches have been characterized using Fourier transform infrared spectroscopy, nuclear magnetic resonance, and thermogravimetric analysis/differential scanning calorimetry. The pitches have been graphitized at 2500 °C and characterized by X-ray diffraction and transmission electron microscopy for graphitic quality assessment. The Synpitch showed larger crystallites (by over 50%) and markedly better nanostructure compared to the commercial pitch used in this study. The structural differences between the pitches are highlighted here to explain the significantly better graphitic quality of the Synpitch.

Keywords: coal tar pitch; petroleum pitch; graphite; solvent extraction; TEM; FTIR; NMR; TGA; DSC; synthetic pitch

Citation: Gharpure, A.; Vander Wal, R.L.; Pisupati, S. Synthetic Pitch from Solvent Extraction of Coal as a Source for High-Quality Graphite. *C* **2023**, *9*, 56. https://doi.org/10.3390/c9020056

Academic Editor: Cédric Pardanaud

Received: 10 February 2023
Revised: 14 May 2023
Accepted: 25 May 2023
Published: 1 June 2023

1. Introduction

Graphitic carbons have gained importance because of their use as an anode material in energy storage devices. As the graphitic quality of the carbons is a function of starting material composition, large-scale production of graphitic carbon relies on the supply of high-quality precursors. Coal-derived pitches are considered superior precursors due to their high aromaticity compared to petroleum pitches which contain fewer aliphatics and condensed alkylated aromatics. Furthermore, compared to coal, petroleum resources are relatively less abundant given the demand from other competing applications. Meanwhile, the domestic availability of traditional coal tar pitches (CTP) is on the decline [1–4] due to offshoring of the coke production for reasons of environmental policy and economics. Despite their advantages, drawbacks of traditional CTP include their high quinoline insoluble content and relatively low hydrogen content; both impede good mesophase formation. These shortcomings stem from the traditional thermal devolatilization methods for obtaining coal tars and pitches—which also face challenges regarding product yield, energy efficiency, and associated environmental impact. Therefore, new strategies need to be investigated for obtaining graphitizable precursors from abundant coal reserves.

A good quality graphite precursor should have both aromatic and aliphatic components. The planarity of the aromatic molecules provides an advantage for proper alignment and growth of the mesophase via condensation reactions, yet some crosslinking still occurs. In contrast, pure aliphatic precursors first need to go through dehydroaromatization to produce aromatics which increases the extent of crosslinking that can occur during carbonization. Having an aliphatic component along with aromatics in a pitch can help form

a better mesophase. This is because higher hydrogen content increases the fluidity of the molecules helping them orient better by slowing aromatization and concatenation [5,6]. Additionally, the transferable aliphatic hydrogen also helps stabilize the transient free radicals, reducing intermolecular reactivity, which limits crosslinking and promotes an anisotropic liquid crystal system. This is why upgraded precursors (with higher H/C content) potentially have a higher graphitic quality after heat treatment.

This paper demonstrates an environmentally clean and economical solvent extraction process to produce high-quality synthetic pitch (Synpitch) from domestically sourced raw materials. The process involves using a recycled coal tar distillate cut to extract coal pyrolysis products at moderately high temperature and pressure (~425 °C at 600 psig). The temperature used is significantly lower than that used in metallurgical coke production (~1000 °C [7,8]) netting energy savings. The pressure helps the dissolution of the lighter hydrogen-rich fragments in the extract. The presence of hydrogen-rich species in the solvent stabilizes the pyrolyzing coal radicals and also solvates the coal molecular fragments. The pitch produced from such a tar (extract) would have an overall higher H/C ratio and aliphatic content compared to the pitch prepared with traditional methods. The key advantages of this process over the well-known direct liquefaction processes (Bergius, NEDOL, H-Coal, SRC-II, EDS, Shenhua process, etc.) are that the addition of a catalyst and a large amount of hydrogen are not necessary [9–12]. Another advantage is that this continuous process requires substantially lower pressure than the conventional Bergius process which requires up to 3000 psig. The Synpitch also contains a significantly lower amount of non-graphitizable quinoline insolubles, ash content, and environmentally unfriendly pyrene derivative compounds compared to conventional pitches.

This paper examines the graphitization potential of Synpitch compared to a petroleum pitch obtained from a leading commercial pitch vendor. The distinctions between the two pitches have been characterized using Fourier transform infrared spectroscopy (FTIR), nuclear magnetic resonance (NMR), thermogravimetric analysis (TGA), and differential scanning calorimetry (DSC). The pitches have been graphitized (GR) at 2500 °C, and their graphitic quality has been assessed using transmission electron microscopy (TEM) and X-ray diffraction (XRD).

2. Materials and Methods

2.1. Materials

The Synpitch was prepared in a 10 gal laboratory setup at West Virginia University using a scheme outlined in Figure 1. The ground West Virginia bituminous coal [13,14] was suspended in ~33 wt% middle-cut coal tar distillate (a widely researched commodity [15–18]) and transferred to an autoclave reactor. This slurry was heated at 425 °C at 600 psig with constant stirring for 1 h. The reactor products were then flashed to an expansion tank through a condenser. The devolatilized products were cooled to 200 °C, and any insoluble material was filtered out in a de-ashing system. The extract was then distilled to obtain a pitch with the desired softening point (~120 °C). The process does not need additional solvent as it can be recycled, and the makeup solvent can be obtained from the coal itself. This patented process is described elsewhere [19–21] and is currently licensed to Penncara Energy. A commercial petroleum pitch from a leading vendor having a softening point of 174 °C (K174) was obtained as a comparison to the Synpitch. Table 1 provides the primary characterization of the selected pitches.

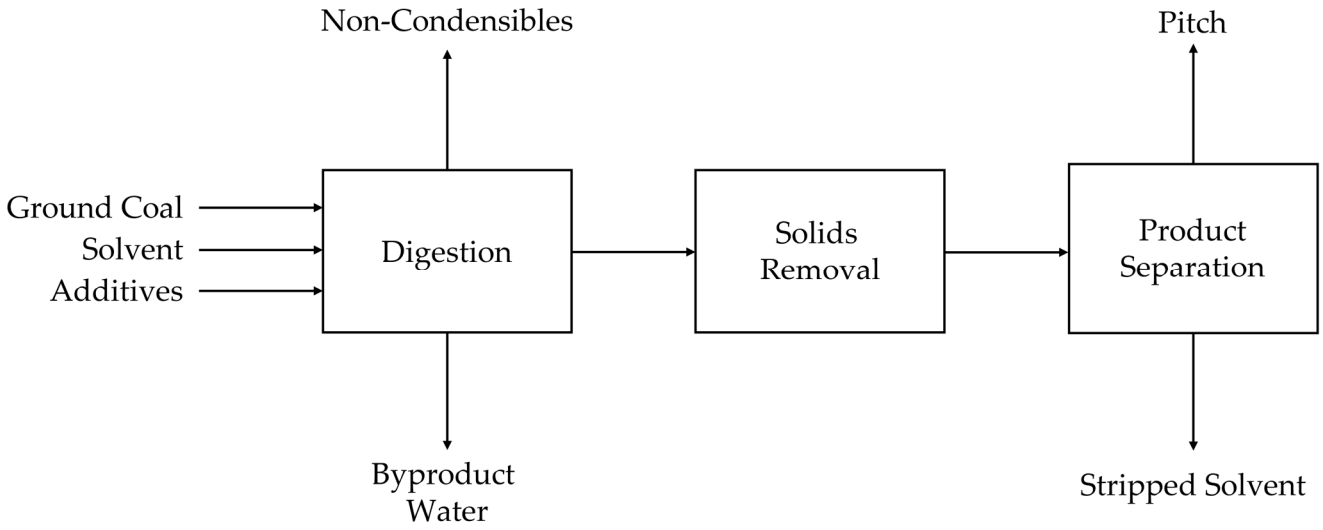

Figure 1. Simplified block flow diagram of the laboratory Synpitch process.

Table 1. Pitch characterization.

Sample	Softening Point (°C)	Q.I. (wt%)	T.I. (wt%)	Coking Value (wt%)	Ash Content (wt%)	Moisture Content (wt%)
K174	174	8	20	48	0.1	0.1
Synpitch	120	2.8	30.9	51.7	0.2	0.1

2.2. Fourier Transform Infrared Spectroscopy

Fourier transform infrared spectroscopy (FTIR) was used to gain insights into the aromaticity, functional groups, and molecular framework of the pitches. The measurements were made by taking 800 scans in ATR mode using a Bruker Vertex 70v (Bruker, Billerica, MA, USA) equipped with a liquid-nitrogen-cooled mercury-cadmium-telluride (MCT) detector on as-received pitches. A linear background was subtracted in each peak region, and the integrated areas of the fitted peaks were used for evaluating differences between the pitches.

2.3. Nuclear Magnetic Resonance

^{13}C CP/MAS experiments were performed on a Bruker Avance III HD 11.75 T spectrometer (499.87 MHz for 1H; 125.70 MHz for ^{13}C) employing a 4 mm triple resonance CP/MAS probe operated in the double resonance mode. The samples were spun at 10 KHz after packing in a 4 mm zirconia rotor. In these experiments, 1024 scans were acquired with a recycle delay of 5 s. The CP contact time was set to 2 ms. An RF pulse of 83 kHz was used for both proton excitation and decoupling. The RF amplitude for CP was ~70 KHz.

Although Bloch decay or single-pulse excitation (SPE) studies are now recognized as being more accurate for absolute quantification, they are less sensitive and highly time-consuming [22,23]. According to some studies, certain components like non-protonated aromatics may get underestimated in cross-polarization/magic-angle spinning (CP/MAS) measurements, especially for samples containing paramagnetic components or free radicals (such as coals) [23–25]. Others show that CP gives comparable results to SPE in pitches [25]. It is important to note that our samples contain little paramagnetic impurities, and the main interest is not absolute quantification but only the relative distinctions between the two pitches. The structure determined using CP and SPE are close when dealing with highly aromatic samples such as the ones used in this study [23]. Here, CP/MAS has been used for expedient characterization of the pitches.

2.4. Thermogravimetric Analysis/Differential Scanning Calorimetry

Comparative thermogravimetric analysis/differential scanning calorimetry (TGA-DSC) analysis of the pitches was performed using a NETZSCH STA-449 Jupiter TGA-DSC, Selb, Germany. These measurements were performed at conditions that were used to obtain carbonized samples for graphitization. Around 10–15 mg of as-received pitches were heated from 40 °C to 600 °C at 25 °C/min under an inert N_2 flow of 100 mL/min.

2.5. Carbonization and Graphitization

The pitches were loaded in alumina boats and inserted in a Thermolyne® 21,100 horizontal tube furnace (Thermo Fisher Scientific, Waltham, MA, USA) holding an alumina tube. The carbonization was carried out at 600 °C for 3 h under a continuous flow of inert argon. The obtained cokes were loaded in graphite crucibles and graphitized using a Centorr Vacuum Industries' series 45 graphitization furnace at 2500 °C for 1 h. An inert atmosphere was maintained by removing air from the graphitization furnace by multiple pump-down cycles (to less than 100 millitorrs) followed by argon backfills and a continuous purge.

2.6. X-ray Diffraction

X-ray diffraction (XRD) has been used for the bulk-scale analysis of lattice parameters of the GR-pitches. Measurements were carried out using a Malvern PANalytical Empyrean diffractometer equipped with a Cu source (λ = 1.54 Å), para-focusing optics, and a pixel 3D detector. The instrument was calibrated using the silicon reference standard material, and the spectrum was scanned from 2θ of 5° to 90°. The MDI JADE® (International Centre for Diffraction Data, Newtown Square, PA, USA) was used for peak deconvolution and quantification. The lattice parameters were calculated using Scherrer's equation on the lowest residual fits.

2.7. Transmission Electron Microscopy

The GR-pitches samples were ground and suspended in ethanol. The solution was then sonicated using a sonication horn for 5 min and drop-casted on 300 mesh C/Cu lacey TEM grids. Transmission electron microscopy (TEM) was performed using an FEI TalosTM F200X microscope (Thermo Fisher Scientific) equipped with a FEG source providing 0.12 nm resolution. The instrument was operated at 200 kV, and TEM images were taken at various magnifications from 10 kX to 630 kX. The local crystallinity of individual flakes/particles was assessed by selected area electron diffraction (SAED) patterns.

3. Results

3.1. FTIR

Figure 2 shows an FTIR spectra overlay of K174 versus Synpitch, and the inset shows a magnified region indicating the differences in aromaticity. The deconvolution of FTIR spectra is shown in the Supplementary Materials. The aromaticity index (I_{Ar}) of the pitches was calculated from the relative peak areas of the aromatic and aliphatic hydrogen bands in the ~2800–3100 cm^{-1} region as

$$\frac{(\text{Peak Area})_{\sim 3050\ cm^{-1}}}{(\text{Peak Area})_{\sim 3050\ cm^{-1}} + (\text{Peak Area})_{\sim 2920\ cm^{-1}}}$$

The higher aliphatic component of Synpitch is clearly evident in the relative peak areas of aromatic and aliphatic C–H stretches (inset figure), with an aromaticity index of 0.73 versus 0.82 for K174. The lower relative area of the peak around ~750 cm^{-1} compared to other out-of-plane aromatic C–H peaks in the 700–900 cm^{-1} region suggests that Synpitch contains more pericondensed aromatic structures compared to K174. The other peaks around 3420 cm^{-1}, 3520 cm^{-1}, and in the oxygen functional group region (1000–1800 cm^{-1}) indicate a significantly higher proportion of oxygenated compounds in K174 compared to Synpitch. The relative distribution of aliphatic hydrogens in $–CH_2–$ versus $–CH_3$ structures

(2800–2980 cm^{-1} and 1370–1480 cm^{-1}) has been used to evaluate the relative proportion of cyclic versus straight chain aliphatic structures in pitches [26]. However, that may not be a correct interpretation because those $–CH_2–$ and $–CH_3$ peaks do not necessarily arise from aliphatics and could be from aliphatic substituents on aromatics (e.g., ethylbenzene). In fact, if we compare the standard FTIR spectrum of propane and ethylbenzene, it becomes clear that $–CH_2–$ and $–CH_3$ peaks could also contribute to aliphatic substituents on aromatics. A contribution from aliphatic substituents on aromatics could be more dominant than that from pure aliphatics, specifically in the case of highly aromatic (i.e., having very little amount of pure aliphatics) pitches being examined here. Therefore, Synpitch likely has a significantly higher proportion of alkylated and hydrogenated aromatics than K174.

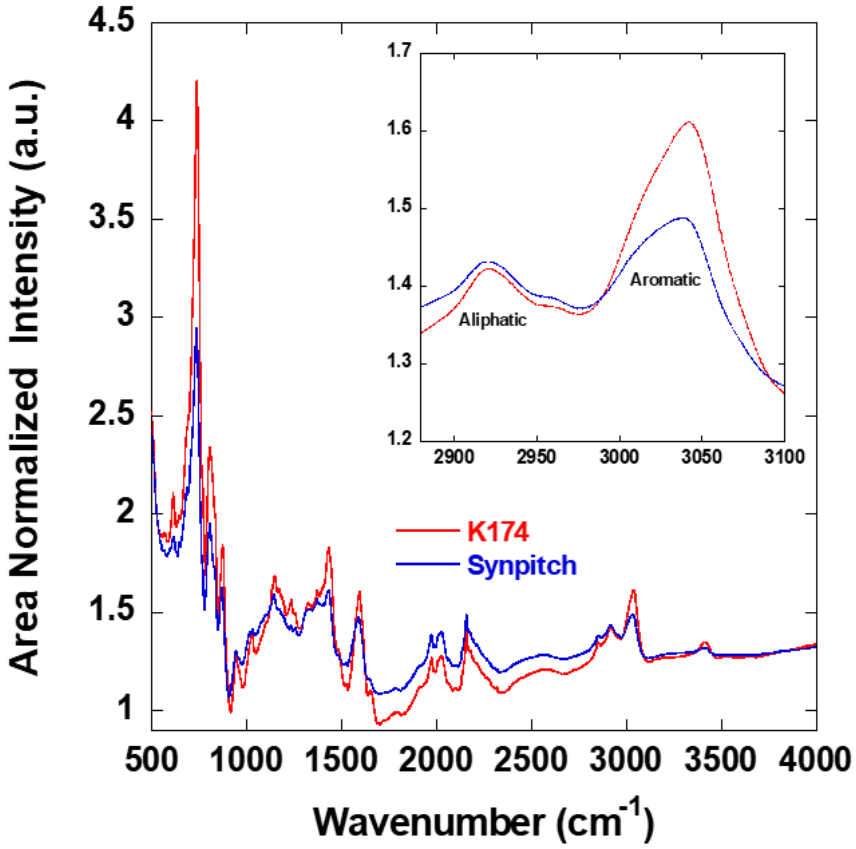

Figure 2. Overlay of FTIR spectra of as-received K174 versus Synpitch.

3.2. NMR

The chemical shifts of different kinds of aliphatic and aromatic carbons have been researched [25,27,28]. Figure 3a shows an overlay of ^{13}C CPMAS NMR spectra from as-received K174 versus Synpitch with the inset showing a magnified aliphatic region (~49.3–17 ppm). The spinning sidebands are labeled as SS. The higher aliphatic content of the Synpitch compared to K174 is clearly evident in the inset figure. Furthermore, a higher proportion of the aliphatic content in Synpitch is in the form of a bridge between two aromatics (~34–49.3 ppm) compared to methyl carbons (~23–17 ppm). Figure 3b shows the magnified aromatic region indicating that compared to K174, Synpitch has a significantly higher ratio (more than double) of pericondensed aromatics (~129.5–108 ppm) to catacondensed aromatics (~160–129.5 ppm). For quantifying the differences between the pitches, the peaks were deconvoluted after subtracting a linear background, and the ratios based on integrated peak areas (including SS) are reported in Table 2. The deconvolution of NMR spectra is shown in the Supplementary Materials.

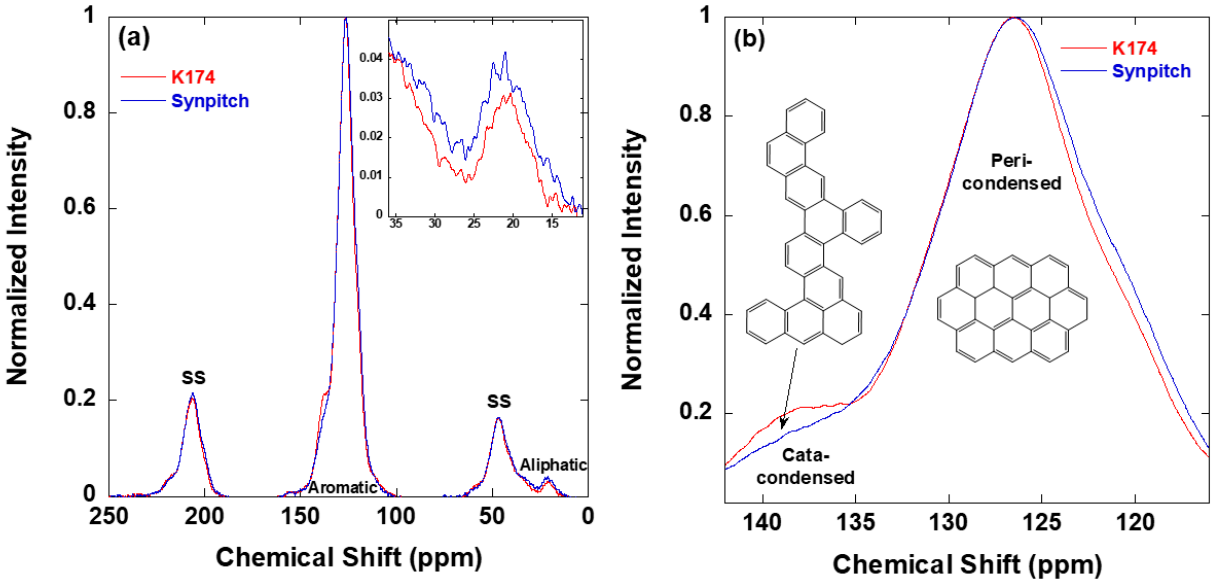

Figure 3. An overlay of ^{13}C CPMAS NMR spectra of as-received K174 versus Synpitch (**a**) broad range and (**b**) magnified range showing differences in Pericondensed/Catacondensed ratio.

Table 2. Normalized integrated data from ^{13}C CPMAS NMR of as-received pitches.

Compound Class	Aromatic/Aliphatic	Pericondensed/Catacondensed	Bridge/Methyl
K174	0.97	6.3	0.76
Synpitch	0.86	13.4	0.89

3.3. TGA-DSC

Figure 4 shows an overlay of (a) thermogravimetry (TG) and derivative thermogravimetry (DTG), (b) DSC and derivative DSC (DDSC), and (c) DTG and DDSC for K174 versus Synpitch. The DSC peaks below 300 °C are not accompanied by weight loss and, therefore, can be attributed to phase transitions. The DSC peak around ~80 °C is likely the transition of the pitch to a viscoelastic state. The DSC peak between 100 °C and 200 °C in Figure 4b is due to the glass transition temperatures (related to the softening point) of the pitches. The DSC curves confirm the lower softening point of the Synpitch consistent with its higher aliphatic content compared to K174. The weight loss for both pitches starts after 300 °C and is associated with various endo- and exothermic processes occurring simultaneously such as devolatilization, dehydrogenation, molecular arrangement, aromatization, condensation, etc. Synpitch has higher rates of weight loss in the lower temperature segment (300–450 °C), which is related to higher aliphatic content and corresponding higher devolatilization extent as seen in Figure 4a. In contrast, K174 shows a higher weight loss rate in the higher temperature segment (450–600 °C). Additionally, the temperature of the maximum rate of weight loss (highest intensity peak of the DTG curve in Figure 4a) is distinctly different for the pitches. Synpitch and K174 show the maximum rate of weight loss at ~475 °C and ~525 °C, respectively. The lower temperature band (<500 °C) is seen in samples mainly comprising mesophase, while the higher temperature band is associated with reactions involving molecules that require higher temperature for structural changes and that do not form mesophase easily [29]. This suggests that Synpitch has a substantially higher content of mesophase-forming molecules. The peaks above 500 °C are nominally associated with polymerization and the onset of cracking [30]. Synpitch shows a noteworthy DTG peak separation at ~550 °C as evident by the shoulder accompanied by a large exothermic DDSC peak while K174 shows just a broad DTG peak in that region (Figure 4c). This peak separation for Synpitch could be indicative of relatively demarcated onset temperatures for different reactions in Synpitch. In contrast, the broad single symmetric DTG

peak for K174 suggests that all reactions co-occur. This suggests that some polymerization and cracking reactions in Synpitch could be "delayed" (occur at a different stage at a higher temperature), which is recognized in pitches showing higher radical stabilization through hydrogen transfer. Such behavior for Synpitch would be highly beneficial for mesophase formation as the longer duration of fluidity allows for better alignment and orientation of the molecules.

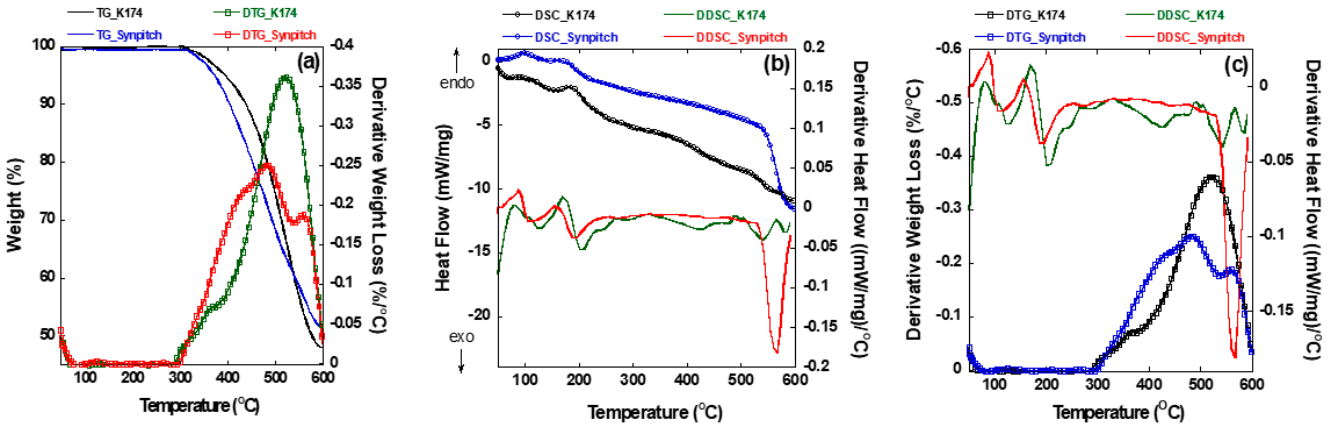

Figure 4. An overlay of (**a**) TG and DTG, (**b**) DSC and DDSC, and (**c**) DTG and DDSC for K174 versus Synpitch.

3.4. X-ray Diffraction

Figure 5 shows an overlay of the XRD pattern for GR-K174 versus GR-Synpitch with the inset figures showing magnified 002 and 110 peaks corresponding to stacking height (L_c) and in-plane crystallite size or lateral dimension of the graphene layer (L_a), respectively. It is evident that GR-Synpitch has a significantly smaller full width at half maximum for the 002 and 110 peaks indicating markedly larger crystallite size compared to GR-K174. Table 3 provides XRD-derived crystallite lattice parameters for GR-K174 versus GR-Synpitch. The L_a and L_c values of GR-Synpitch are 60% and 54% higher than GR-K174, respectively. The better definition of 101 peaks in Synpitch also indicates substantially better crystalline order in the third (c-axis) direction.

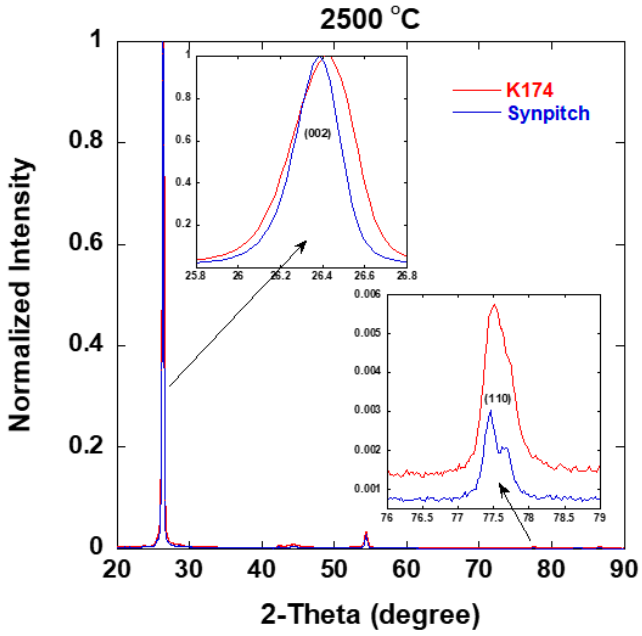

Figure 5. XRD overlay for GR-K174 versus GR-Synpitch.

Table 3. XRD-derived crystallite lattice parameters for GR-K174 versus GR-Synpitch.

Lattice Parameter | Compound	GR-K174	GR-Synpitch
d_{002} [Å]	3.37	3.37
L_c (using 002) [nm]	24.08	37.01
L_a (using 100) [nm]	38.79	55.80
L_a (using 110) [nm]	72.02	114.97

3.5. Morphology and Nanostructure Assessment

Figures 6 and 7 show panels of TEM images for GR-K174 and GR-Synpitch, respectively. GR-K174 and GR-Synpitch both show thin flake morphology with a particle size of ~2–10 µm. GR-K174 showed some non-uniformity within most flakes/particles, as evidenced by darker striped regions in Figure 6a,b. The darker regions showed better graphitic quality, while the remaining regions had relatively less structured lamellae leading to the observed diffraction contrast. GR-Synpitch showed rather better uniformity within the particles, with such dark stripes evident mainly at the locations of folds on the flake, as shown in Figure 7a–c. Some amorphous content was also seen in GR-K174 (Figure 6d,f–i), which was absent in GR-Synpitch. GR-Synpitch also showed substantially better nanostructure compared to GR-K174. The nanostructure of GR-K174 consists of a zig-zag undulated lamellae, as seen in Figure 6e–h. A few particles showed a straight contiguous lamellae structure, as seen in Figure 6c. On the other hand, almost all surveyed GR-Synpitch particles showed long contiguous lamellae with good stacking extending over tens of nanometers, as evident in Figure 7d–h.

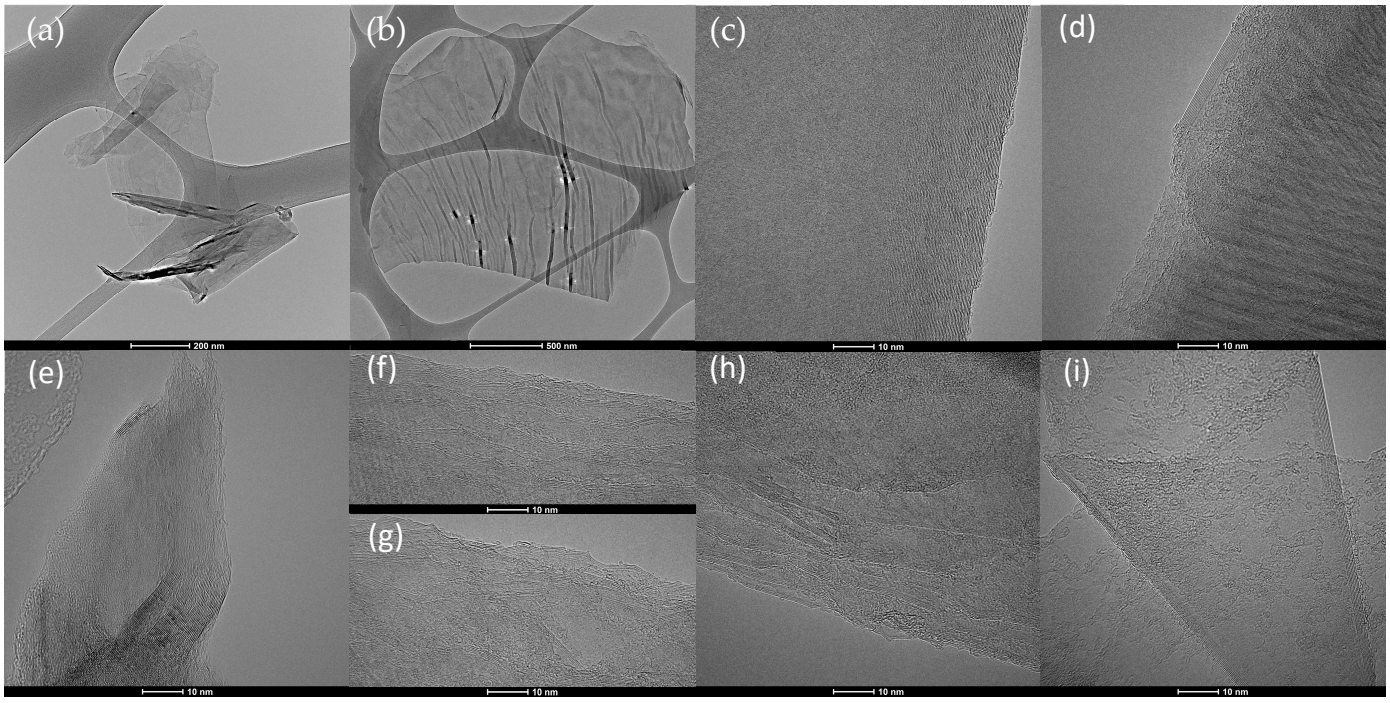

Figure 6. A panel showing TEM and HRTEM images of GR-K174.

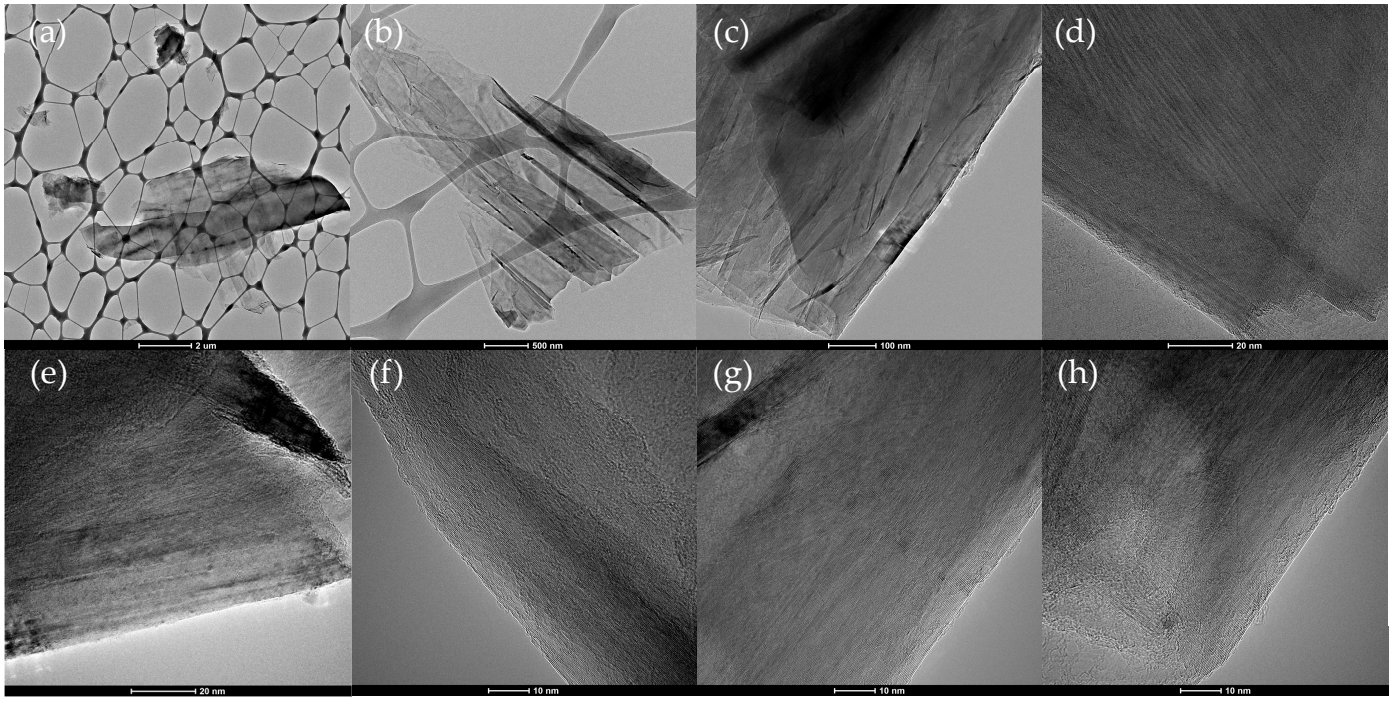

Figure 7. A panel showing TEM and HRTEM images of GR-Synpitch.

4. Discussion

Synpitch has a significantly higher aliphatic component compared to K174, which is evident in the lower softening point of Synpitch compared to K174. A higher percentage of the aliphatic content in Synpitch is present on the aromatics as the bridge between two aromatic domains and as alkyl substituents. This is highly beneficial for mesophase formation as it keeps pitch molecules in the fluid phase for longer, allowing them to orient better and reducing crosslinking by limiting intermolecular reactivity via hydrogen transfer reactions. Low QI and ash content (<1%) of the Synpitch are advantageous for good mesophase formation. TGA-DSC suggests that Synpitch has significantly higher mesophase-forming molecules and stays in a fluid state for a longer duration compared to K174, which should be highly beneficial for better alignment and orientation. Synpitch also contains significantly higher pericondensed aromatics, which can merge/condense better, while K174 contains more catacondensed aromatics, which condense haphazardly given their branched and/or zig-zag structure. This could be why GR-K174's nanostructure shows zig-zag lamellae and smaller crystallites. K174 also has a significantly higher oxygenated compound content which contributes to crosslinking. On the other hand, GR-Synpitch shows longer and straighter lamellae with larger stacking height. This should be highly beneficial for lithium-ion batteries given the comparative ease of lithium intercalation in the uniform and extended galleries. The markedly larger crystallites in the GR-Synpitch should also provide better mechanical, electrical, and thermal properties compared to GR-K174. The Synpitch studied in this work is obtained from bituminous coal. A similar process could also be applied using lower-rank coals to obtain graphitizable synthetic pitches, which will be studied subsequently.

5. Conclusions

This work assesses the graphitization potential of synthetic pitch obtained from a novel coal solvent extraction process. The process provides benefits of lower temperature, pressure, and hydrogen requirement. The obtained coal-derived pitch contains upgraded (higher H/C) compounds with a higher proportion of pericondensed aromatics and lesser environmentally unfriendly pyrene derivative compounds compared to petroleum and traditional coal tar pitches. These along with lower QI and ash content are favorable

characteristics for a pitch to be highly graphitizable. Indeed, the Synpitch was substantially better at yielding a 50% larger crystallite size compared to the commercial petroleum pitch. The nanostructure of GR-Synpitch was also remarkably better with long contiguous and well-stacked lamellae compared to zig-zag undulated/tortuous lamellae in the commercial petroleum pitch.

Supplementary Materials: The following supporting information can be downloaded at: https://www.mdpi.com/article/10.3390/c9020056/s1.

Author Contributions: Conceptualization, A.G. and S.P.; methodology, A.G.; software, A.G.; validation, A.G. and R.L.V.W.; formal analysis, A.G.; investigation, A.G.; resources, R.L.V.W. and S.P.; data curation, A.G.; writing—original draft preparation, A.G.; writing—review and editing, A.G., R.L.V.W. and S.P.; visualization, A.G.; supervision, R.L.V.W.; project administration, R.L.V.W.; funding acquisition, R.L.V.W. All authors have read and agreed to the published version of the manuscript.

Funding: Acknowledgment is made to the donors of the American Chemical Society Petroleum Research Fund for support of this research.

Institutional Review Board Statement: Not applicable.

Acknowledgments: Authors gratefully thank Alfred Stiller from Penncara for providing Synpitch to Penn State.

Conflicts of Interest: The authors declare no conflict of interest.

References

1. MarketWatch. Coke Market Size by Regional Industry Growth, Statistics & Forecast. Available online: https://www.marketwatch.com/press-release/coke-market-size-by-regional-industry-growth-statistics-&-forecast-2019-05-18 (accessed on 17 December 2019).
2. Kraynik, C.E. Strategies for a Declining North American Coal Tar Supply. In *National Coal Industrial Meeting*; Koppers Industries Inc., Technical Center: Pittsburgh, PA, USA, 2005.
3. United Nations Statistics Division. Coke Oven Coke Production. Available online: http://data.un.org/Data.aspx?d=EDATA&f=cmID%3AOK (accessed on 6 October 2022).
4. Conner, J.R. Metallurgical Coal. Available online: http://www.flatheadmemo.com/north_fork_coal/Coal/News/coke.html#:~:text=Foundries_use_coke_as_a,the_production_of_calcium_carbide (accessed on 6 October 2022).
5. Mochida, I.; Kudo, K.; Takeshita, K.; Takahashi, R.; Suetsugu, Y.; Furumi, J. Modifying Carbonization Properties of Pitches. 1. Conversion of Benzene-Insoluble Matter of Coal-Tar Pitch into Graphitizable Carbon. *Fuel* **1974**, *53*, 253–257. [CrossRef]
6. Edwards, I.A.S.; Marsh, H.; Menendez, R. *Introduction to Carbon Science*; Butterworth-Heinemann: Oxford, UK, 2013.
7. U.S. Environmental Protection Agency. Coke Production. Available online: https://www3.epa.gov/ttnchie1/old/ap42/ch12/s02/bgdocs/b12s02.pdf (accessed on 6 October 2022).
8. Clean Air Council. Coke and How Its Made. Available online: https://pacokeovens.org/what-is-coke/ (accessed on 6 October 2022).
9. Taylor, W.F.; Hall, H.J. *Future Synthetic Fuels. A Scientific and Technical Applications Forecast. Final Report*; Government Research Lab, Exxon Research and Engineering Co.: Linden, NJ, USA, 1975.
10. Stevens, T.; Udall, M.K. *Increased Automobile Fuel Efficiency and Synthetic Fuels: Alternatives for Reducing Oil Imports*; Congress of the U.S., Office of Technology Assessment: Washington, DC, USA, 1982.
11. Baughman, G.L. *Synthetic Fuels Data Handbook*; Cameron Engineers: Denver, CO, USA, 1978.
12. Shui, H.; Cai, Z.; Xu, C. Recent Advances in Direct Coal Liquefaction. *Energies* **2010**, *3*, 155–170. [CrossRef]
13. Davis, A.; Glick, D.C.; Hatcher, P.G.; Mitchell, G.D. Maintenance of the Coal Sample Bank & Database, 11/99, 2841095. 1999. Available online: https://www.osti.gov/servlets/purl/827653 (accessed on 5 January 2021).
14. Choi, C.Y.; Muntean, J.V.; Thompson, A.R.; Botto, R.E. Characterization of Coal Macerals Using Combined Chemical and NMR Spectroscopic Methods. *Energy Fuels* **1989**, *3*, 528–533. [CrossRef]
15. Sun, Z.; Zhang, W. Chemical composition and structure characterization of distillation residues of middle-temperature coal tar. *Chin. J. Chem. Eng.* **2017**, *25*, 815–820. [CrossRef]
16. Seshadri, A.S.; Cronauer, D.C. Characterization of coal-derived liquids by 13C nmr and FT-ir spectroscopy: Fractions of middle and heavy distillates of SRC-II. *Fuel* **1983**, *62*, 1436–1444. [CrossRef]
17. Fairbridge, C.; Kriz, J.F. Hydroprocessing of coal-derived middle distillate. *Fuel Sci. Technol. Int.* **1986**, *4*, 171–189. [CrossRef]
18. Caramão, E.B.; Gomes, L.M.F.; Bristoti, A.; Lancas, F.M. Characterization op medium distillate cut (100–230 °C) oil from high-ash "mina do leão" brazilian coal tar. *Pet. Sci. Technol.* **1990**, *8*, 173–190. [CrossRef]
19. Dadyburjor, D.; Biedler, P.R.; Chen, C.; Clendenin, L.M.; Katakdaunde, M.; Kennel, E.B.; King, N.D.; Magean, L.; Stansberry, P.G.; Stiller, A.H. *Production of Carbon Products Using a Coal Extraction Process*; West Virginia University: Morgantown, WV, USA, 2004.

20. Kennel, E.; Chen, C.; Dadyburjor, D.; Heavner, M.; Katakdaunde, M.; Magean, L.; Mayberry, J.; Stiller, A.; Stoffa, J.; Yurchick, C. *Development of Continuous Solvent Extraction Processes for Coal Derived Carbon Products*; West Virginia University: Morgantown, WV, USA, 2009.
21. Kennel, E.B.; Stansberry, P.G.; Stiller, A.H.; Zondlo, J.W. *Method of Producing Synthetic Pitch*; West Virginia University: Morgantown, WV, USA, 2012.
22. Franz, J.A.; Garcia, R.; Linehan, J.C.; Love, G.D.; Snape, C.E. Single-Pulse Excitation 13C NMR Measurements on the Argonne Premium Coal Samples. *Energy Fuels* **1992**, *6*, 598–602. [CrossRef]
23. Maroto-Valer, M.M.; Andrésen, J.M.; Rocha, J.D.; Snape, C.E. Quantitative Solid-State 13C Nmr Measurements on Cokes, Chars and Coal Tar Pitch Fractions. *Fuel* **1996**, *75*, 1721–1726. [CrossRef]
24. Muntean, J.V.; Stock, L.M. Bloch Decay Solid-State Carbon-13 NMR Spectroscopy of the Samarium Iodide-Treated Argonne Premium Coals. *Energy Fuels* **1991**, *5*, 765–767. [CrossRef]
25. Andresen, J.M.; Luengo, C.A.; Moinelo, S.R.; Garcia, R.; Snape, C.E. Structural Uniformity of Toluene-Insolubles from Heat-Treated Coal Tar Pitch as Determined by Solid State 13C Nmr Spectroscopy. *Energy Fuels* **1998**, *12*, 524–530. [CrossRef]
26. Alcañiz-Monge, J.; Cazorla-Amorós, D.; Linares-Solano, A. Characterization of Coal Tar Pitches by Thermal Analysis, Infrared Spectroscopy and Solvent Fractionation. *Fuel* **2001**, *80*, 41–48. [CrossRef]
27. Díaz, C.; Blanco, C.G. NMR: A Powerful Tool in the Characterization of Coal Tar Pitch. *Energy Fuels* **2003**, *17*, 907–913. [CrossRef]
28. Twigg, A.N.; Taylor, R.; Marsh, K.M.; Marr, G. The Characterization of Coal Tar Pitches Used in Electrode Binder Manufacture by n.m.r. Spectroscopy. *Fuel* **1987**, *66*, 28–33. [CrossRef]
29. Blanco, C.; Prada, V.; Santamaría, R.; Bermejo, J.; Menéndez, R. Pyrolysis Behaviour of Mesophase and Isotropic Phases Isolated from the Same Pitch. *J. Anal. Appl. Pyrolysis* **2002**, *63*, 251–265. [CrossRef]
30. Manocha, L.M.; Patel, M.; Manocha, S.M.; Vix-Guterl, C.; Ehrburger, P. Carbon/Carbon Composites with Heat-Treated Pitches: I. Effect of Treatment in Air on the Physical Characteristics of Coal Tar Pitches and the Carbon Matrix Derived Therefrom. *Carbon N. Y.* **2001**, *39*, 663–671. [CrossRef]